JOURNAL OF VIROLOGY, Mar. 1994, p. 1271–1282
0022-538X/94/$04.00+0

Vol. 68, No. 3

Herpes Simplex Virus Type 1 DNA Replication and Gene Expression during Explant-Induced Reactivation of Latently Infected Murine Sensory Ganglia

G. B. DEVI-RAO,[1] D. C. BLOOM,[2] J. G. STEVENS,[2] AND E. K. WAGNER[1]*

Department of Molecular Biology and Biochemistry, University of California, Irvine, Irvine, California 92717,[1] and Department of Microbiology and Immunology, UCLA Medical School, Los Angeles, California 90024[2]

Received 16 August 1993/Accepted 16 November 1993

Infectious virus assays and PCR amplification of DNA and RNA were used to investigate herpes simplex virus DNA replication and gene expression in two murine in vitro models for virus reactivation. We examined latent infections with wild-type (*wt*), precisely defined latency-associated transcript-negative (LAT$^-$) mutants, and LAT$^+$ rescuants of these mutants of the 17*syn*$^+$ strain of virus in both murine trigeminal and lumbosacral ganglia and of the KOS(M) strain in the latter. In explants of ganglia latently infected with the LAT$^-$ mutant of strain 17*syn*$^+$ virus, a reduction in number of cultures exhibiting cytopathic effects due to virus reactivation and measurable delays in virus recovery were observed compared with *wt* or the LAT$^+$ rescuant. This LAT-specific effect was not seen in explants of lumbosacral ganglia latently infected with mutants derived from the KOS(M) strain of virus. Although there was appreciable variation between individual animals, no significant difference between LAT$^+$ and LAT$^-$ virus in time of onset of viral DNA replication in explanted ganglia was seen with use of either virus strain. There was a slight decrease in the relative amount of viral DNA recovered compared with internal cellular controls in latently infected ganglia harboring the LAT$^-$ mutant of 17*syn*$^+$ compared with the *wt* virus or the LAT$^+$ rescuant. This reduced relative amount ranged from 0 to as much as 50% but averaged 20%. Such differences were not seen in infections with KOS(M)-derived mutants. In contrast, although expression of productive-cycle transcripts could be detected within 4 h following explant cultivation of latently infected ganglia, no differences between LAT$^+$ and LAT$^-$ viruses could be seen. As discussed, these data place specific constraints on possible models for the role of LAT expression in in vitro reactivation systems.

The alphaherpesviruses are neurotropic and establish latent infections in sensory ganglia (8, 36). Many of these viruses, including herpes simplex virus types 1 and 2 (HSV-1 and -2), pseudorabies virus, and bovine herpesvirus, express a very limited region of their genomes during this latent phase of infection. To date, the best-characterized example is HSV-1, for which such transcripts are termed the latency-associated transcripts (LATs) (14, 29, 37, 44, 45). These transcripts are expressed as a single 8.5-kb primary transcript from which 2- and 1.4-kb stable introns and (presumably) unstable processed forms are derived (10, 12).

In humans and several in vivo models, reactivation of HSV results in the appearance of infectious virus at the site of initial primary infection (8, 15, 17, 18, 23, 33, 35, 36). It is generally agreed that LAT expression has a significant role in this phenomenon, but the precise mechanism of this involvement is unknown (2, 3, 13, 19, 24, 31, 34, 43). Although described (6, 32), murine models for efficient in vivo reactivation of HSV-1 have been generally difficult to exploit; however, infectious virus can be recovered with high efficiency upon explant and culture of latently infected murine sensory ganglia. Such explant cultivation has been extensively used as an in vitro reactivation model to take advantage of the relative convenience of murine latency models. Although the efficiency and/or kinetics of virus recovery have been shown to be influenced by LAT expression in several laboratories (2, 3, 24, 34), many basic parameters of the system, including details of viral genome transcription and replication as well as the influence of virus strain and anatomical site of latent infection, remain unknown.

In this report, we have described the results of a careful comparative analysis of two in vitro murine models of reactivation of HSV from latent infection: the eye model, in which latent virus can be recovered by explant cultivation of trigeminal ganglia, and the footpad infection model, in which virus establishes latent infection in murine lumbosacral ganglia. We have used the wild-type (*wt*) KOS(M) and 17*syn*$^+$ strains of HSV-1 as well as precisely defined LAT$^-$ mutants and LAT$^+$ rescuants of these mutants in these studies. In agreement with reports from other laboratories, we observe a slight but significant delay in the recovery of infectious virus from trigeminal ganglia infected with the LAT$^-$ mutant of the 17*syn*$^+$ virus compared with ganglia infected with either the LAT$^+$ rescuant or *wt*. This delay was also observed in explant cultivation of murine lumbosacral ganglia latently infected with 17*syn*$^+$ but not with KOS(M) mutants.

We also have begun a careful molecular analysis of HSV-1 DNA replication and gene expression especially with respect to LAT expression in these two murine model systems, using the sensitivity of the PCR. We measured the recovery of HSV DNA in latently infected ganglia relative to the recovery of two single-copy cellular genes, the adipsin and actin genes. Although there was appreciable variation between individual animals in signal strength for HSV DNA detected, a net increase in the relative amount of viral DNA compared with cellular DNA could be reproducibly detected within 48 h following explant. In contrast to the results of virus recovery

* Corresponding author. Mailing address: Department of Molecular Biology and Biochemistry and Program in Animal Virology, University of California, Irvine, Irvine, CA 92717. Phone: (714) 856-5370. Fax: (714) 856-8551. Electronic mail address: EWAGNER@UCI.EDU.

assays, we detected no time difference between LAT$^+$ and LAT$^-$ viruses in the onset of viral DNA replication in explants of either trigeminal or lumbosacral tissue. In ganglia infected with the 17*syn*$^+$ virus, however, at time of explant averaged about 80% of the ratio seen with LAT$^+$ infections; this difference was not seen in dorsal root ganglia latently infected with KOS(M) virus.

Productive-cycle transcripts could be also be detected with PCR no more than 4 h following explant of either trigeminal or lumbosacral ganglia latently infected with both the LAT$^+$ and LAT$^-$ genotypes of either virus used. Because of these results, it seems possible that differences in viral recoveries seen in the assays described above are related to numbers of neurons latently infected and not to a role of LAT in in vitro reactivation per se. The accompanying report compares and contrasts these observations with those obtained in an in vivo rabbit reactivation model (4).

MATERIALS AND METHODS

Cells and virus. Rabbit skin cells, mouse embryo fibroblasts, and murine neuroblastoma cells were cultured in minimal essential medium containing 5% fetal calf serum and antibiotics as described previously (10). HSV-1 strains 17*syn*$^+$ and KOS(M) were used along with engineered mutants of both strains containing a deletion of the 203-bp *Pst*I-*Pst*I fragment encompassing the TATA box and transcription start site within both copies of the LAT promoter. This deletion corresponds to bases 118664 through 118866 of the long internal repeat of the 17*syn*$^+$ strain, the corresponding bases in the long terminal repeat, and equivalent sites in the KOS(M) strain. The generation of the deletion [KOS/29(LAT$^-$)] of the KOS(M) strain of virus has been described, as have general methods for screening and confirming the identity of recombinants (11). This mutant was rescued to generate KOS/29Pr(LAT$^+$) by cotransfection of infectious KOS/29(LAT$^-$) DNA with a 2.3-kb *wt* KOS(M) *Hpa*I-*Sph*I fragment (spanning locations equivalent to bases 117007 to 119286 of the 17*syn*$^+$ sequence). We generated 17ΔPst(LAT$^-$) virus by recombining the 5.8-kb *Aat*II fragment spanning bases 115853 to 121547 from which the *Pst*I fragment had been deleted with *wt* DNA. Finally, the 17Pr(LAT$^+$) rescue virus was generated by cotransfection of infectious 17ΔPst(LAT$^-$) DNA with a 900-base *wt* 17*syn*$^+$ DNA fragment spanning a *Not*I site at base 118438 and the *Bst*EII site at base 119194.

Replication of mutants in mouse tissue. Primary mouse embryo fibroblasts were maintained at 38.5°C; 5×10^6 cells were infected at a multiplicity of infection (MOI) of 0.05 PFU per cell. Virus was adsorbed for 1 h; monolayers were washed twice with supplemented medium and overlaid with medium containing 12% fetal bovine serum. Infection mixtures were incubated at 38.5°C in a 5% CO_2 atmosphere. At the indicated times, cells were harvested by scraping into medium and frozen at −70°C. The virus was released by two rounds of freeze-thawing, and the samples were titrated on confluent monolayers of rabbit skin cells.

For in vivo replication, groups of four mice were inoculated with 5×10^2 PFU of the appropriate virus into the left cerebral hemisphere. Virus titers in brains were determined as previously described (42). Briefly, at the times indicated, three mice inoculated with each virus were killed, and their brains were removed and frozen at −70°C. The brains were then homogenized as a 10% (wt/vol) suspension and centrifuged for 5 min at 3,000 × *g* at 4°C. The resulting supernatant was assayed for virus on rabbit skin cell monolayers.

Latent infections and explant reactivation of murine sensory nerve ganglia. General methods have been described elsewhere (39, 40, 46). Latent infections in the trigeminal ganglia of 8-week-old Swiss Webster mice were established as follows. Mice were anesthetized with 1.5 mg of sodium pentobarbital, and the corneas were scarified by making three horizontal and three vertical strokes across the cornea with a scalpel blade. Each cornea was then inoculated with 10^6 PFU of *wt* 17*syn*$^+$, 17ΔPst(LAT$^-$), or 17Pr(LAT$^+$) virus in 5 μl. The inoculum was distributed over the surface of each cornea by closing the eyelids and rubbing over the eye in a circular motion. Latently infected trigeminal ganglia were removed 21 days following inoculation.

For latent infections of lumbosacral ganglia with KOS(M) virus and derivatives (38), 6-week-old Swiss Webster mice were inoculated with 5×10^6 PFU of HSV-1 in each rear footpad. For infections with strain 17*syn*$^+$ and derivatives, mice were infected with 5×10^3 PFU per foot. In both cases, the feet were injected with 1 M saline approximately 4 h prior to inoculation as described previously (7). We have previously shown that compared with strain 17*syn*$^+$, KOS(M) is not neuroinvasive. When the viruses are inoculated into footpads at equivalent dosages, the amount of KOS(M) recoverable from spinal ganglia at later time intervals is significantly less than the amount of 17*syn*$^+$ (40). In an attempt to ensure establishment of latent infection in maximal numbers of neurons, mice were infected with the highest concentration of virus consistent with survival of a significant number of animals. In the 17*syn*$^+$ experiments, this corresponds to 1 50% lethal dose; for KOS(M), undiluted virus stocks could be used. Two to three weeks later, animals were killed, L1 through L5 spinal ganglia on each side were dissected, and groups of 12 to 20 ganglia were pooled and either directly snap frozen in liquid N_2 for latent DNA or RNA or incubated in culture medium for times varying from 4 to 48 h and then snap frozen. The time of incubation was scored as time of in vitro reactivation.

To score for reactivation of virus in vitro, L4 and L5 spinal ganglia were removed from 10 mice for each virus tested, cocultivated individually in 24-well Costar dishes on rabbit skin cell monolayers for 18 to 30 days, and scored daily for reactivation. Cultures were fed every other day, and wells were observed daily and scored as positive when virus-induced cytopathology appeared. For the ΔPst(LAT$^-$) viruses, the genotype of reactivating virus was confirmed by diagnostic Southern blot analysis of purified viral DNA from positive wells.

Extraction of DNA and RNA from cells and tissue. Productively infected cell RNA was isolated at 6 h following infection at an MOI of 5 PFU per cell. Low-MOI infection of cultured cells was done with cultures of 8×10^5 cells infected with 8×10^2 PFU of virus (MOI, 10^{-3}). DNA was extracted from single trigeminal ganglia, pools of 20 to 24 spinal ganglia, or cultures of 8×10^5 cells by digestion with 250 μg of proteinase K (Sigma) in 1% sodium dodecyl sulfate containing buffer comprising 150 mM NaCl, 10 mM Tris, and 25 mM EDTA (pH 7.4) as described previously (19).

RNA was isolated from cells or tissue essentially as described previously (10, 39) by extraction with guanidinium isothiocyanate; extracted material was extensively digested with RNase-free DNase, and RNA was then recovered by centrifugation for 16 h at 36,000 rpm in a Beckman SW41 rotor through a 5.7 M CsCl cushion.

PCR amplification of DNA and RNA. Primer sets for PCR amplification were chosen by searching the appropriate regions of the sequence of the 17*syn*$^+$ strain of HSV-1 (26), using a published computer algorithm (25); primer sets used are shown in Table 1. Standard conditions were amplification of

TABLE 1. PCR primers used to detect HSV-1 DNA replication and viral transcripts in latently infected and explanted ganglia

Viral gene	Primer pair[a]	Sequence location[b] (bp)	Kinetic class	Size of PCR product (bp)
5′-LAT	5′-CGGCGACATCCTCCCCCTAAGC-3′	118888–118909	Latent	149
	5′-GACAGACGAACGAAACATTCCG-3′	119036–119015		
LAT-exon	5′-GTGTCGTTCAACAAAGACGCCG-3′	119431–119452	Latent	149[c]
	5′-TCTTCCTCCTCTGCCTCTTCC-3′	121530–121510		
3′-LAT	5′-GGTGAAACCAACAGAGCACGGC-3′	126377–126398	Latent	160
	5′-CCGGGGTACGTCTGGAGGAGCG-3′	126537–126516		
α4 (ICP4)	5′-GGCGGGAAGTTGTGGACTGG-3′	127308–127289	α	138
	5′-CAGGTTGTTGCCGTTTATTGCG-3′	127171–127192		
α27 (U_L54)	5′-TTTCTCCAGTGCTACCTGAAGG-3′	114922–114943	α	283
	5′-TCAACTCGCAGACACGACTCG-3′	115204–115184		
Ribonucleotide reductase (U_L39)	5′-GACAGCCATATCCTGAGC-3′	90730–90747	β	221
	5′-ACTCACAGATCGTTGACGACCG-3′	90929–90950		
DNA polymerase (U_L30)	5′-GAACACGGACTATTACTTCTCC-3′	66274–66295	β	227
	5′-CAAAGGCTCTATGCAACATTCG-3′	66500–66479		
VP5 (capsid) (U_L19)	5′-TGAACCCCAGCCCCAGAAACC-3′	35564–35544	βγ	149
	5′-CGAGTAAACCATGTTAAGGACC-3′	35416–35437		

[a] The topmost primer in each pair is the upstream (mRNA sense) primer; the bottom is the downstream (mRNA antisense) primer. Primers were chosen by use of a computer algorithm described elsewhere (25).

[b] Locations are based on the complete sequence of the 17*syn*$^+$ strain of HSV-1 (26). Only the locations in the long and short internal repeats are indicated for LAT and α4 genes.

[c] Size of product for spliced primary transcript; unspliced transcript will yield a 2,099-bp product.

10% of the total extracted RNA or 5% of the total DNA sample for 30 cycles, using Perkin-Elmer Amplitaq polymerase (Norwalk, Conn.) with buffers supplied. Cycling reactions were performed with an M.J. Research Corp. (Cambridge, Mass.) thermal cycler. Cycles were as follows: (i) denaturation at 94°C for 30 s; (ii) annealing at 5°C below the melting temperature of the primers (or actin-specific primers for mixed PCR reactions) for 30 s; and (iii) extension for 60 s at 72°C. The final cycle was terminated with a 10-min extension period at 72°C. Aliquots of 0.2 μCi of [α-^{32}P]dCTP were included in most reaction mixes for the visualization of products by autoradiography. Aliquots of 20% of the amplification products (corresponding to amplification of 1% of the original DNA sample or 2% of the original RNA sample) were fractionated on 6% polyacrylamide gels (20 by 16 by 0.15 cm) running in Tris-borate-EDTA buffer. Run times were 1.5 to 2 h at 250 V and 87 mA. Gels were vacuum dried and exposed overnight for amplification of DNA or overnight at −70°C with intensifying screens for products of RNA amplification. When used, densitometry was performed with a Bio-Rad model 620 video densitometer.

Nucleic acids were prepared for amplification as follows. Samples of the total DNA extracted from tissue were used directly in a 100-μl reaction mix. For cDNA amplification of RNA, total RNA from samples was subjected to oligo(dT)-primed cDNA synthesis, using reverse transcriptase and buffers supplied with the Invitrogen (San Diego, Calif.) cDNA cycle kit. In some control experiments, cDNA was generated from random hexamer primers. Direct RNA PCR was performed as recommended by the supplier, using a GeneAmp RNA PCR kit (Perkin-Elmer Cetus). RNA was reverse transcribed with recombinant *Taq* DNA polymerase, using the antisense primer at 70°C in the presence of $MnCl_2$, and the amplification procedure was carried out on this cDNA by adding upstream primer and $MgCl_2$ after chelating the Mn^{2+} ions.

Specificity of amplified DNA product was confirmed by hybridization of Southern blots of PCR products. Blotting and basic hybridization methods have been described elsewhere (41, 46, 47). Specific probes were oligonucleotides whose sequence was within the amplified product; nonspecific probes were oligonucleotides with sequences representing another amplified gene.

RESULTS

Recovery of virus from explanted latently infected murine ganglia. Previous studies by us and others have demonstrated that LAT$^-$ mutants replicate and are as neurovirulent as their LAT$^+$ parents or rescuants (reviewed in references 29 and 45). Specific experiments comparing multistep replication of *wt*, ΔPst(LAT$^-$) mutant, and LAT$^+$ rescue viruses following low-MOI infection in mouse embryo fibroblasts in vitro and mouse brains in vivo are shown in Fig. 1. Growth properties of the viruses are identical under both conditions; thus, the PFU/50% lethal dose ratio calculated with the formula of Reed and Muench (28) for the KOS/29(LAT$^-$) mutant was 180 ± 45, and that for the KOS/29Pr(LAT$^+$) rescuant was 200 ± 45. Similar data were obtained with 17ΔPst(LAT$^-$) and 17Pr(LAT$^+$) viruses; the ratios were 40 ± 20 for 17ΔPst-(LAT$^-$) and 60 ± 20 for 17Pr(LAT$^+$) virus.

We measured the appearance of infectious virus in explanted ganglia latently infected with the ΔPst(LAT$^-$) mutants, the LAT$^+$ rescuants, and *wt* variants of both the KOS(M) and 17*syn*$^+$ viruses. Although there was variation between individual experiments, within a given experiment, no difference could be seen either in the time of appearance of infectious virus or in the number of positive ganglia in cultured lumbosacral ganglia infected with *wt*, LAT$^+$, and LAT$^-$ KOS(M) virus (Fig. 2A and B). In contrast to these results, fewer spinal ganglia from mice infected with 17ΔPst(LAT$^-$) reactivated, and the time of appearance of cytopathology was delayed compared with explants of the LAT$^+$ rescuant (Fig. 2C). This effect was also seen in trigeminal ganglia (Fig. 2D). Similar results were obtained when the ΔPst(LAT$^-$) virus was compared with *wt* 17*syn*$^+$ (data not shown).

Semiquantitative detection by PCR of limiting amounts of HSV DNA. We next wished to determine the time of onset of detectable viral DNA replication in explanted ganglia. We used PCR amplification to detect and estimate the relative

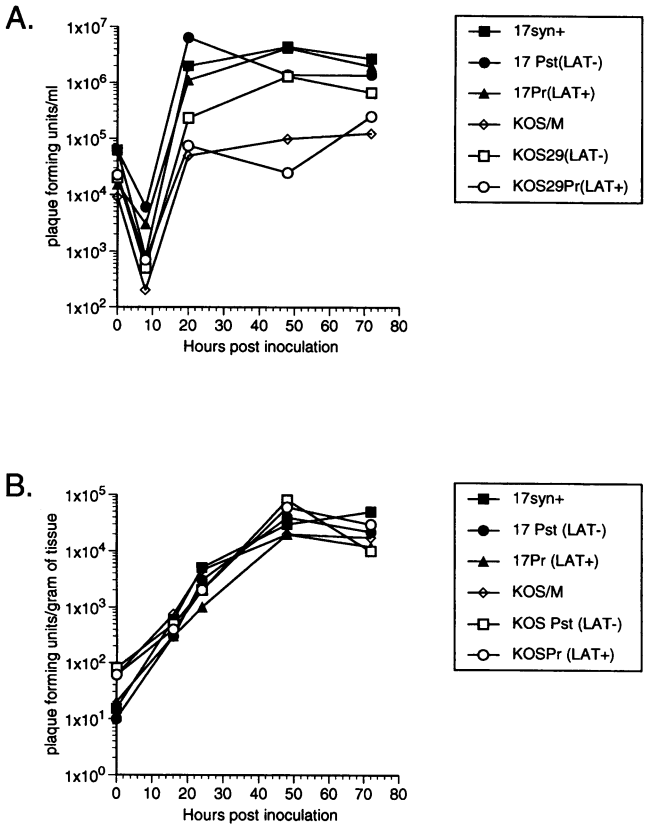

FIG. 1. Recovery of HSV in productively infected cells and explanted latently infected murine ganglia. (A) Mouse embryo fibroblasts were infected with an MOI of 0.05 PFU per cell. Monolayers were overlaid with minimal essential medium containing glutamine and 10% fetal bovine serum and incubated at 38.5°C for the times indicated before assay of virus recovery. (B) Six-week-old female Swiss Webster mice were inoculated intracerebrally with 5×10^2 PFU of virus. At the indicated times postinoculation, three mice per virus were sacrificed, brains were removed, and virus titer was determined.

amounts of viral compared with cellular DNA present at various times after explant. To validate the specificity, sensitivity, and semiquantitative nature of the approach, we carried out a number of control experiments as follows.

We chose primer sets (Table 1) specific for the following viral genes: α4 (ICP4), α27 (ICP27), U_L30 (DNA polymerase), U_L39 (ICP6, ribonucleotide reductase), and U_L19 (VP5, the major capsid protein). These primers were chosen so that they could be used to examine viral transcription following reactivation as well as viral DNA replication. To obviate problems with mRNA degradation in oligo(dT)-primed cDNA synthesis, primer sequences for genes expressed during productive infection were confined to the 3′ termini of the specific transcription units. The first two genes encode important transcriptional regulatory proteins expressed immediately following infection, U_L30 and U_L39 are early (β) proteins normally expressed immediately following HSV α gene expression in most cultured cells, and the major capsid protein is encoded by a prototype βγ (leaky-late) transcript which is expressed prior to viral DNA replication but at maximal rates following DNA replication. Taken together, the transcripts encoding these proteins represent both various kinetic classes of viral gene products and viral functions which are important in productive

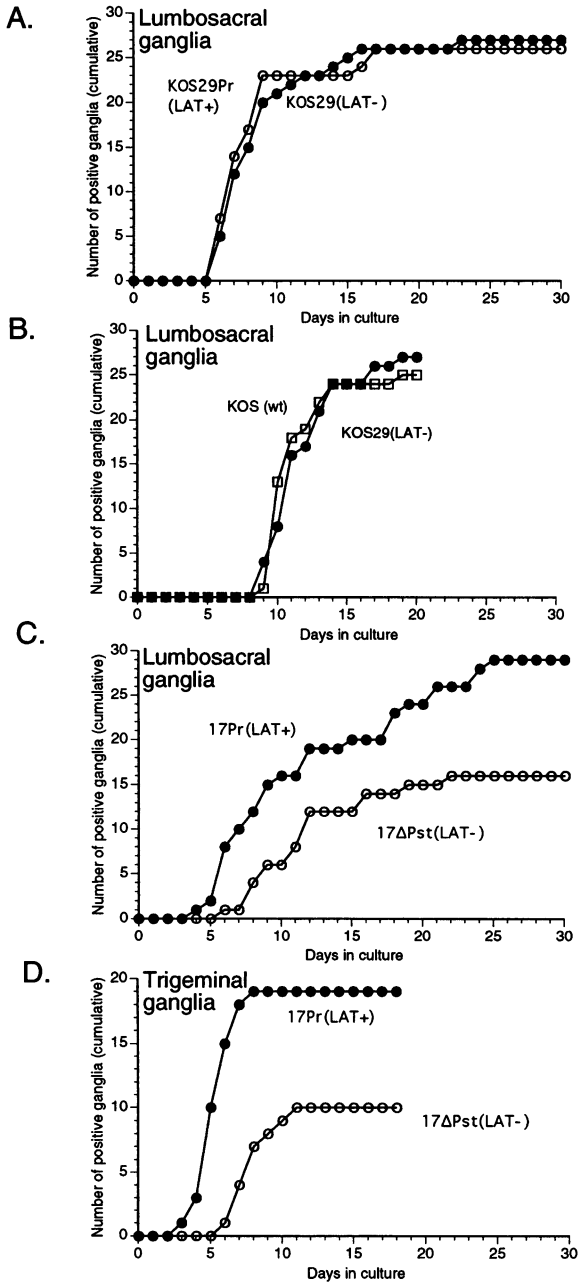

FIG. 2. Virus recovery from explanted murine sensory nerve ganglia latently infected with LAT^- and LAT^+ mutants of HSV. (A) Mice were infected with 5×10^6 PFU of the KOS/29(LAT^-) or KOS/29Pr(LAT^+) virus per rear footpad; 14 days later, L4 and L5 spinal ganglia were dissected from each mouse and cultivated individually on monolayers of rabbit skin cells. Individual ganglia were scored for induced cytopathic effects, and cumulative numbers were plotted versus day first observed. (B) The same experiment was carried out with *wt* KOS(M) and KOS/29(LAT^-) viruses. (C) The same experiment was carried out with 17Pr(LAT^+) and 17ΔPst(LAT^-) viruses. Mice were infected with 5×10^3 PFU per footpad. (D) A similar experiment was carried out by infecting 10^6 PFU of 17Pr(LAT^+) and 17ΔPst(LAT^-) viruses into mouse eyes and explanting the ganglia after 21 days.

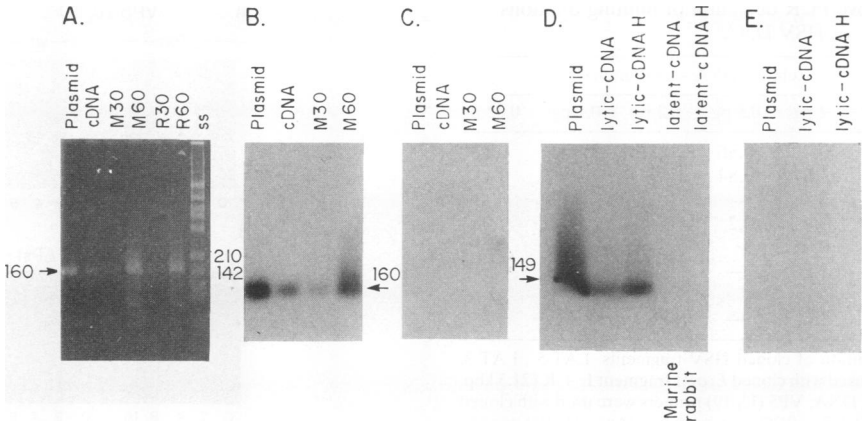

FIG. 3. Specificity of PCR primers used to detect HSV DNA replication and transcription in latently infected ganglia. All primers used are listed in Table 1. (A) Ethidium bromide-stained gel of the amplified products obtained by using the PCR 3′ primers with 50 ng of cloned *Eco*RI fragment E + K (21.3 kb, 0.721 to 0.864 map units) DNA (plasmid) standard samples of oligo(dT)-primed cDNA from lytically infected cells (cDNA), or standard samples of oligo(dT)-primed cDNA made from RNA isolated from latently infected murine ganglia (M30 and M60) or latently infected rabbit ganglia (R30 and R60 [4]). The samples were amplified for 30 cycles except for those marked 60, in which case 10% of the 30-cycle product was subjected to a second round of 30 cycles of amplification. The size markers (ss) were from cloned *Hin*fI-digested polyomavirus DNA spanning bases 400 (*Pst*I) to 4635 (*Bam*HI). Sizes are indicated in bases. (B) A Southern blot of the products was hybridized with a specific oligonucleotide for an internal portion of the amplification product (5′-GTCACACGTCACGTCATCCACC-3′). (C) An identical blot was hybridized with an oligonucleotide specific for an internal portion of the LAT-5′ amplification product. (D) A Southern blot of standard 30-cycle amplification products from 50 ng of *Bam*HI fragment M (5.3 kb, 0.222 to 0.258 map units) containing the VP5 (U_L19 gene) (plasmid), oligo(dT)- or random hexamer-primed cDNA from lytically infected cell RNA (lytic-cDNA and lytic-cDNA H), or the amplification product of oligo(dT)- or random hexamer-primed cDNA of latently infected murine and rabbit neuronal RNA (latent-cDNA and latent-cDNA H). Hybridization was with a probe specific for the internal sequence of the amplification product (5′-GGCGGACGTCCAACAACTCGGT-3′). (E) Hybridization of an identical blot with probe specific for the PCR 3′ product.

infection in cultured cells (44). Primer sequences were derived from the sequence of the 17*syn*$^+$ strain of HSV-1, but we experimentally confirmed the fact that these sequences detected DNA and RNA from the KOS(M) strain with equivalent sensitivity.

Finally, we also chose three primer sets to represent different portions of the primary LAT transcription unit: (i) a primer set specific for the 5′ end (LAT-5′); (ii) a primer set bridging the splice donor and acceptor signals in the primary transcript which would produce a small product only from the spliced LAT species resulting from the generation of the LAT intron (10, 12) (LAT-exon); and (iii) a primer set specific for the 3′ end near the polyadenylation signal (LAT-3′).

PCR product specificity was assessed with cloned DNA fragments and confirmed by Southern blot hybridization of specific internal oligonucleotide probes to unlabeled products amplified from cDNA generated from RNA isolated from latently infected sensory nerve ganglia or productively infected cells. Oligonucleotides from the interior of the primer sets hybridized efficiently with the specific PCR product but not with products generated by other primer sets. Examples for LAT-3′ and VP5 primer sets are shown in Fig. 3. The LAT-3′ product can be readily visualized in stained gels of amplification products of DNA and of cDNA generated from productively infected cells or latently infected ganglia (Fig. 3A). Hybridization of the amplification product of plasmid DNA and cDNA from productively infected cells and murine ganglia with an oligonucleotide specific to the amplified region produced a readily detectable signal (Fig. 3B); however, hybridization with an oligonucleotide specific to the LAT-5′ amplified region did not (Fig. 3C). The VP5 primer set amplified cloned DNA and cDNA generated from RNA isolated from productively infected cells but not latently infected ganglia (Fig. 3D). Hybridization with the nonspecific oligonucleotide was negative (Fig. 3E).

The sensitivity of the PCR primers as semiquantitative probes was measured directly and indirectly. Direct measurement was carried out by limiting-dilution analysis of cloned DNA standards. As has been reported by many others (22, 30; reviewed in reference 20), different primer sets display different sensitivities for detecting limiting amounts of DNA. Within a narrow range of concentrations of HSV DNA, signal intensity could be roughly correlated with amounts of DNA present; however, the response was often not strictly linear. For this reason, quantitation of PCR signal intensities could only be estimated. Summary data for several primer sets are shown in Table 2, and specific examples for which cloned KOS(M) DNA standards were used are shown in Fig. 4. With most primer sets, the amplification product from 0.02 pg (2×10^{-14} g) or less of cloned DNA sample subjected to PCR under our standard conditions of 30 cycles of amplification in a 100-μl reaction mix containing 0.2 μCi of [^{32}P]dCTP could be readily detected upon overnight exposure. On the basis of the size of the specific HSV fragment cloned, this corresponds to the ability to detect fewer than 1,000 genomes.

Experimental confirmation of both the sensitivity of the PCR methods used as well as the ability to reliably measure relative increases in viral DNA recovered from small amounts of infected tissue was obtained with the following control experiments, examples of which are shown in Fig. 5 and Table 3. Cultures of rabbit skin, mouse embryo fibroblasts, or mouse neuroblastoma cells were infected with an MOI of 10^{-3} PFU per cell with either the KOS(M), 17*syn*$^+$, or ΔPst(LAT$^-$) virus. DNA was extracted, diluted to correspond to 10 productively infected cells, and subjected to PCR analysis. In all experiments, DNA replication as assayed by a significant increase in amplified DNA signal intensity in the infected cell mixture could be detected by 4 to 8 h postinfection. Although individual variation in various experiments was observed, as shown in the examples illustrated, no consistent differences

TABLE 2. Quantitative PCR detection of limiting dilutions of HSV DNA[a]

Probe	Relative DNA signal intensity[b]					
	10 pg	2 pg	0.5 pg	0.2 pg	0.1 pg	0.02 pg
5′-LAT	1.31	0.7	0.56	0.19	0.11	0.12
3′-LAT	1.72	1.57	0.84	0.5	—[c]	0
α4	1.02	0.3	—	0.17	—	0
α27	0.6	0.4	0.2	0.16	—	0.05
DNA polymerase	0.4	0.05	0	—	—	0
Ribonucleotide reductase	—	1.2	—	0.8	—	0.5
VP5	—	1.2	—	0.8	—	0.2

[a] DNA was obtained by dilution of cloned HSV fragments. LAT-5′, LAT-3, and α27 (U_L54) primers were used with cloned *Eco*RI fragment E + K (21.3 kbp, 0.721 to 0.864 map units [mu]) DNA; VP5 (U_L19) primers were used with cloned *Bam*HI fragment M (5.3 kbp, 0.222 to 0.258 map units) DNA; α4 (ICP4)-specific primers were used with *Xho*I-*Eco*RI fragment P + I/E + K (8.4 kbp; 0.808 to 0.864 map units) DNA; and ribonucleotide reductase (U_L39)-specific primers were used with *Hin*dIII fragment L DNA (8.8 kbp; 0.592 to 0.647 map units).

[b] Based on densitometry of overnight exposures. Variations are ±25% in separate experiments; units are arbitrary.

[c] —, dilution was not measured.

were seen between either strain of *wt* virus and the ΔPst-(LAT$^-$) mutants. Also, no consistent differences were seen in any of the cell lines or with any PCR primer sets used.

HSV DNA replication following explant of latently infected murine sensory ganglia. We used the technology described above to compare the time of onset of viral DNA replication following explant of murine ganglia which had been latently infected with *wt*, ΔPst(LAT$^-$), or LAT$^+$ rescuant virus. All

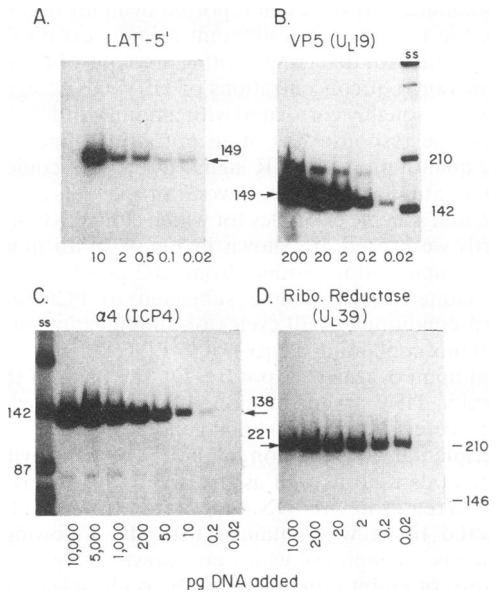

FIG. 4. Quantitation of standard PCR amplification of cloned DNA fragments. The amounts of DNA fragments shown were used with the indicated primer sets, using standard conditions described in Materials and Methods. (A) LAT-5′ primers were used with cloned *Eco*RI fragment E + K DNA. (B) VP5 (U_L19) primers were used with cloned *Bam*HI fragment M DNA. ss, size standards. (C) α4 (ICP4)-specific primers were used with *Xho*I-*Eco*RI fragment (P + I/E + K; 8.4 kbp; 0.808 to 0.864 map units) DNA. (D) Ribonucleotide reductase (U_L39)-specific primers were used with *Hin*dIII fragment L (8.8 kbp; 0.592 to 0.647 map units) DNA. Sizes are indicated in bases.

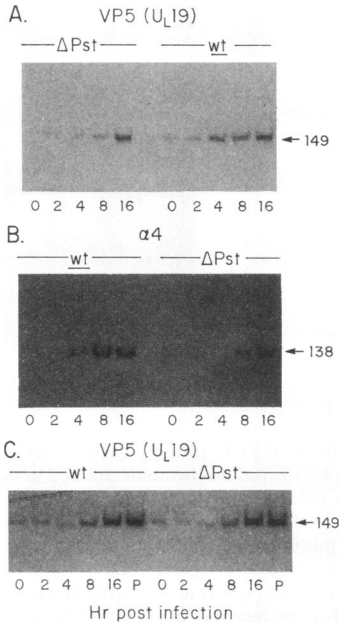

FIG. 5. Onset of DNA replication in cultured cells infected with a low multiplicity of various strains of HSV-1. Cultured cells were infected with an MOI of 10^{-3} PFU of virus per cell and incubated for the times shown prior to DNA extraction and PCR amplification. (A) Infection of rabbit skin cells with *wt* KOS(M) and KOS/29(LAT$^-$) mutants. DNA was primed with VP5 primers. (B) Infection of rabbit skin cells with the 17*syn*$^+$ strain and the 17ΔPst(LAT$^-$) mutant of HSV-1. DNA amplification was primed with α4 primers. (C) Murine neuroblastoma 2A cells were infected with *wt* KOS(M) and KOS/29(LAT$^-$) viruses. The primer set was specific for the VP5 gene. Lanes P are the amplification products of 20 pg of *Bam*HI fragment M DNA. Exposures were overnight without intensifying screens. Sizes are indicated in bases.

experimental procedures were similar. Ganglia were removed from latently infected animals, and DNA was immediately extracted to provide a latent or zero-time control; companion ganglia were then incubated in culture for various times. DNA replication following cultivation was scored by detection of a

TABLE 3. PCR measurement of relative HSV DNA recovery following productive infection at low MOI[a]

Cell type	Time (h) post-infection[b]	Relative HSV DNA signal intensity[c]			
		KOS(M) (*wt*)[d]	KOS/29 (LAT$^-$)	17Pr (LAT$^+$)[e]	17ΔPst (LAT$^-$)[e]
Rabbit skin	0	0.08	0.01	0.1	0.02
	2	0.15	0.12	0.05	0.01
	4	0.5	0.12	0.2	0.05
	8	0.6	0.3	0.5	0.2
	16	0.72	0.6	0.5	0.7
Murine neuroblastoma 2A	0	0.16	0.19	—[f]	—
	2	0.18	0.13	—	—
	4	0.13	0.12	—	—
	8	0.2	0.25	—	—
	16	0.4	0.5	—	—

[a] Quantification of data in Fig. 5.

[b] Following a 30-min virus adsorption period.

[c] Arbitrary units.

[d] VP5 (U_L19) primer set.

[e] α4 primer set.

[f] —, not measured.

TABLE 4. Levels of HSV DNA recovered from explanted latently infected murine sensory nerve ganglia[a]

Type of ganglia	Virus	Time (h) postexplant	Relative DNA signal intensity[b]		Ratio, HSV/actin[c]	Avg ratio, HSV/actin[d] ± SE
			HSV	ACTIN		
Lumbosacral	KOS(M) (*wt*)	0	0.72[c]	0.6[c]	1.20	1.23 ± 0.1
		24	0.98[c]	0.65[c]	1.51	1.26 ± 0.15
		48	1.07[c]	0.65[c]	1.65	2.56 ± 0.7
	KOS/29(LAT$^-$)	0	0.82[c]	0.66[c]	1.24	1.07 ± 0.15
		24	1.02[c]	0.66[c]	1.55	1.3 ± 0.1
		48	1.11[c]	0.62[c]	1.79	2.1 ± 0.3
	KOS/29Pr(LAT$^+$)	0	0.84[c]	0.63[c]	1.33	1.1 ± 0.15
		24	0.98[c]	0.61[c]	1.60	1.3 ± 0.2
		48	1.11[c]	0.53[c]	2.09	1.63 ± 0.15
	17ΔPst(LAT$^-$)	0	—[e]	—	—	0.5 ± 0.1
		48	—	—	—	1.6 ± 0.2
	17Pr(LAT$^+$)	0	—	—	—	0.8 ± 0.2
		48	—	—	—	1.9 ± 0.25
Trigeminal	17*syn*$^+$	0	0.31[d]	0.58	0.53	1.15 ± 0.25
		24	0.56	0.52	1.08	1.01 ± 0.15
		48	1.2	0.51	2.35	2.42 ± 0.2
	17ΔPst(LAT$^-$)	0	0.31	0.52	0.57	0.85 ± 0.12
		24	0.13	0.28	0.46	1.2 ± 0.2
		48	1.06	0.40	2.65	1.99 ± 0.25
	17Pr(LAT$^+$)	0	0.58	0.66	0.88	1.18 ± 0.25
		24	0.90	0.67	1.34	1.7 ± 0.2
		48	1.25	0.41	3.05	2.17 ± 0.3

[a] See text and legends to Fig. 6 and 7 for details.
[b] Arbitrary units. DNA was detected by using VP5 (U_L19) and murine actin primer sets in the same reaction.
[c] Data from Fig. 6D and 7D.
[d] Data from at least two separate tissue extractions and at least three separate reactions. Data from Fig. 6 and 7 are not included.
[e] —, data not shown.

significant increase in the intensity of the PCR signal compared with zero-time controls and quantitated by comparison with signals generated from cellular DNA. Primer sets specific for the murine adipsin (21) and actin genes were used for these controls. The two controls provided similar results, but the actin set produced considerably less background and could be coamplified with the HSV VP5 (U_L19) primer set without interference. The actin primer set was as follows: sense, 5′-AAGATCTGGCACCACACCTT-3′; and antisense, 5′-CAAACATTATCTGCGTCATC-3′. This set generates a 124-bp product and was chosen from the published murine actin sequence (1) to represent positions in the murine actin gene equivalent to those in the rabbit actin gene used as a control for the in vivo studies described in the accompanying report (4, 16, 27).

Several experiments were carried out with a variety of HSV primer sets. Data for the results of coamplification of the VP5 and actin primer sets in the same sample (Table 4) can be summarized as follows. In lumbosacral ganglia latently infected with *wt* KOS(M), KOS/29(LAT$^-$), and KOS/29Pr(LAT$^+$) rescuant virus, in a number of experiments, no significant differences in the amount of viral DNA recovered from latently infected ganglia were found at the time of explant. In some experiments, an increase in the amount of viral DNA recovered was just detectable by 24 h following explant, while this increase was clearly and reproducibly detectable by 48 h postexplant in all experiments. Examples of data obtained with several primer sets are shown in Fig. 6.

In similar experiments (Table 4), DNA replication could be readily detected by 48 h after explant of trigeminal ganglia latently infected with *wt* 17*syn*$^+$, 17ΔPst(LAT$^-$), and the 17Pr(LAT$^+$) rescuant. A specific experiment illustrating the results of amplification of several primer sets is shown in Fig. 7. In contrast to the situation with infections with KOS(M) viruses in spinal ganglia, many experiments demonstrated a measurable reduction in the relative amount of viral DNA recovered following explant of ganglia latently infected with the 17ΔPst(LAT$^-$) virus compared with either *wt* 17*syn*$^+$ or the 17Pr(LAT$^+$) rescuant. In various experiments, densitometric analysis indicated that this difference ranged from the *wt* value to as little as 50% of it, with the average reduction being 20%. Similar data were obtained with explants of lumbosacral ganglia (Table 4). This slight reduction in efficiency of establishment of latent infections by LAT$^-$ viruses derived from 17*syn*$^+$ parents could be a factor in the delay and reduction in virus recovery seen in ganglia latently infected with LAT$^-$ virus compared with LAT$^+$ derivatives.

Detection and measurement by PCR of small amounts of HSV transcripts. We also assayed the expression of productive cycle HSV transcripts in explanted ganglia either by direct PCR amplification of total cell RNA or PCR of oligo(dT)-primed cDNA generated from such RNA. The same primer sets used for analysis of DNA replication (Table 1) were employed. Because the amount of viral mRNA present in infected cells varies with time following infection as well as with cell type and conditions of infection, we did not attempt to make quantitative conclusions concerning viral transcripts. As a measure of the sensitivity and specificity of the method, direct RNA PCR was carried out with serial dilutions of productively infected rabbit skin cell RNA. Aliquots of this infected cell RNA (200 μg in total) corresponding to the yield of 100 to 0.1 infected cell (20 ng to 200 pg of RNA) were diluted into 1-μg samples of uninfected hamster or mouse brain RNA and subjected to direct RNA-directed PCR under standard conditions, and 20% of the product was analyzed by gel electrophoresis. Representative data are shown in Table 5; primer sets for LAT-5′, α27 (U_L54), and U_L19 transcripts detected viral RNA from as few as one infected cell. Other

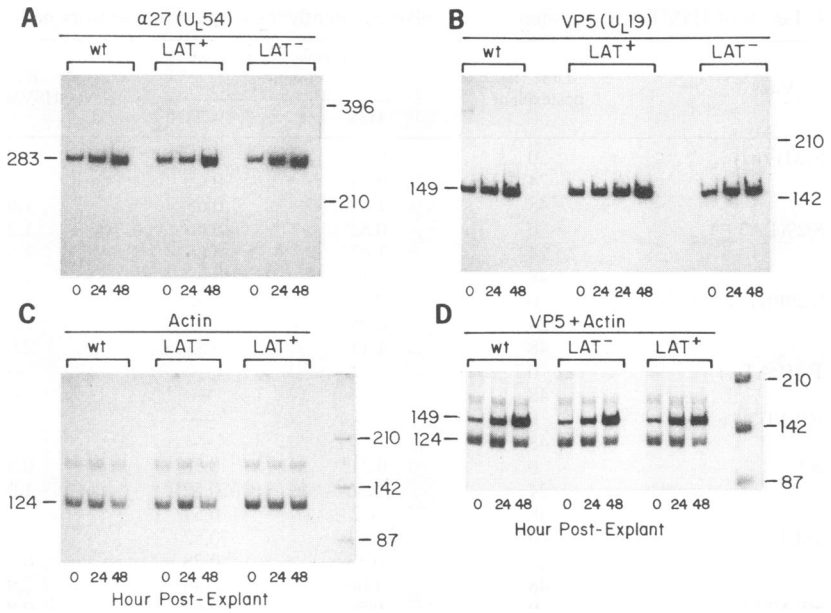

FIG. 6. Onset of HSV-1 DNA synthesis in latently infected murine lumbosacral ganglia following explant cultivation. Ganglia latently infected with *wt* KOS(M), KOS/29(LAT$^-$), and KOS/29Pr(LAT$^+$) viruses were explanted and incubated for the times shown following explant. DNA was subjected to PCR amplification using the primer sets indicated. (A) U_L54 (α27)-specific primers; (B) U_L19 (VP5)-specific primers (the VP5 primer was used with two parallel 24-h samples in the panel shown; (C) murine actin primer set used in a parallel sample; (D) amplification of both VP5- and actin-specific products by inclusion of both primer sets in the same samples. Exposures were overnight without intensifying screens. Sizes are indicated in bases.

primer sets were capable of detecting viral RNA from at least 10 infected cells. The primer set for the spliced LAT product (LAT-exon) did not provide a signal at any dilution of total infected cell RNA used; however, a signal was detected with a sample containing 1 μg of purified poly(A)$^+$ RNA from productively infected cells (data not shown).

The utility of direct PCR for detection of viral RNA from small numbers of productively infected cultured cells was established as follows. Cultures of cells were infected with an MOI of 10^{-3} PFU of HSV-1 KOS(M), 17*syn*$^+$, or the ΔPst-(LAT$^-$) mutant per cell, and whole cell RNA was extracted at various times following infection. An amount corresponding to RNA from 10 infected cells were then subjected to direct PCR. With all viruses tested, HSV RNA could be detected with the α27 (U_L54) primer set as soon as 2 h after infection, while the primer sets for VP5 and U_L39 detected RNA by 4 h. RNase digestion of samples completely abolished the signal.

TABLE 5. Direct PCR detection of limiting amounts of HSV transcripts in productively infected cells[a]

Probe	Relative DNA signal intensity[b]			
	100 cells[c]	10 cells	1 cell	0.1 cell
5′-LAT	1.5	1.3	0.9	0.15
3′-LAT	1.3	0.5	0	0
α4	1.6	1.5	0.17	0
α27	1.6	1.2	0.8	0.05
DNA polymerase	1.4	1.1	0	0
Ribonucleotide reductase	1.5	1.1	0.15	0
VP5	1.7	1.3	0.2	0

[a] Cells were infected with an MOI of 5 PFU per cell as described in Materials and Methods.
[b] Based on densitometry of an overnight exposure. Units are arbitrary and varied ±25% in separate amplifications of the same samples.
[c] Cell equivalents are based on dilution of the original infected cell RNA with uninfected cell RNA.

HSV transcription following explant reactivation of latently infected sensory nerve ganglia. Latently infected murine ganglia were cultured for various times following explant, and RNA was extracted for analysis by either direct PCR or PCR amplification of oligo(dT)-primed cDNA generated from the samples. The two methods gave equivalent results; however, the amplification of oligo(dT)-primed cDNA generally tended to produce less background signal.

Productive cycle transcripts could be detected in ganglia quite soon following explant. Results of an experiment using direct amplification are shown in Fig. 8A. Here, the immediate-early α4 transcript could be detected by 2 h following explant of lumbosacral ganglia latently infected with *wt* KOS(M) virus, while the late (βγ) VP5 (U_L19) transcript was detected by 4 h. The decrease in intensity of the U_L19 signal in the 8-h sample was not seen in other experiments but illustrates the range of variation between various experiments. As expected, signals were completely lost when the samples were treated with RNase.

Since the LAT unit is active during latent infection, the ability to detect transcripts immediately upon explant with the primer set for the 3′ end of the latent-phase transcription unit (LAT-3′) was expected (Fig. 8A). Similar results were seen with use of the LAT-5′ probe; however, no signal was seen when the LAT-exon probe was used (not shown). Since some low-abundance late-productive-phase transcripts also terminate at the polyadenylation signal utilized by the latent-phase transcripts (5, 48), we cannot directly estimate how much of the signal seen with the LAT-3′ primer set later after explant is due to continued LAT expression, but we have previously shown

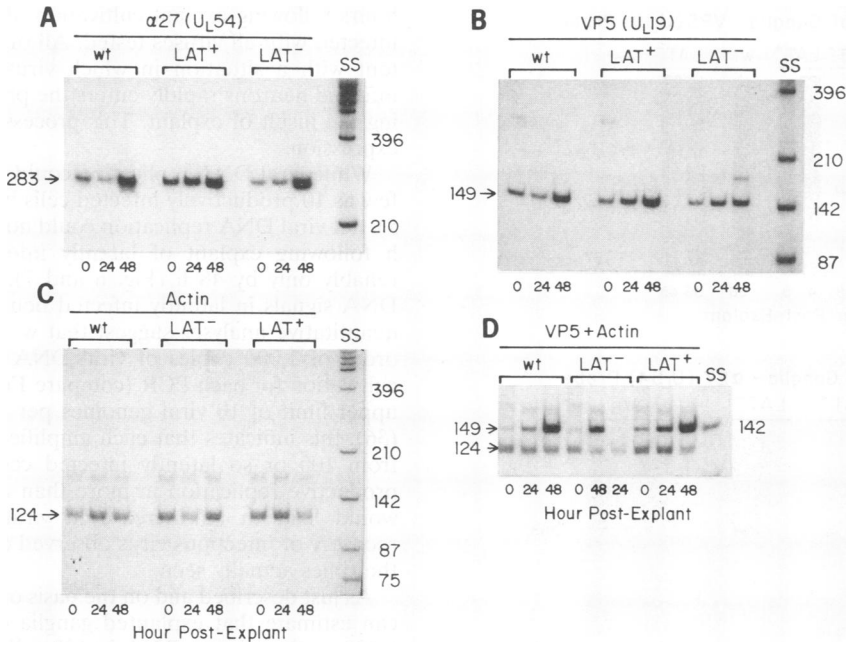

FIG. 7. Onset of HSV-1 DNA synthesis in latently infected murine trigeminal ganglia following explant cultivation. Ganglia latently infected with *wt* 17*syn*$^+$, 17ΔPst(LAT$^-$), and 17Pr(LAT$^+$) viruses were explanted and incubated for the times shown. DNA was subjected to PCR amplification using the primers indicated. (A) U_L54 (α27)-specific primers; (B) U_L19 (VP5)-specific primers; (C) murine actin primer set used in a parallel sample; (D) amplification of both VP5- and actin-specific products by inclusion of both primer sets in the same samples. The 24- and 48-h samples are reversed with the 17ΔPst(LAT$^-$) virus in panel D. Exposures were overnight without intensifying screens. SS, size standards. Sizes are indicated in bases.

that the LAT promoter is active during productive infection in cell culture (10, 41).

Amplification of cDNA and expression of the α27 transcript are shown in Fig. 8B. In this set of experiments, the VP5 primer set provided a detectable signal as early as 1 h following explant, and a stronger signal was detectable at 2 h and later. This variation in time of detection of this βγ transcript between experiments is consistent with the range of variation seen in productive infection of tissue culture cells and likely reflects variations in animals and assay sensitivities.

We then compared the expression of HSV transcripts in explanted murine ganglia infected with LAT$^-$ and LAT$^+$ recombinants. No reproducible differences were seen with either lumbosacral or trigeminal ganglia. Representative data shown in Fig. 9A demonstrate that VP5 (U_L19) mRNA was detectable by 4 h following explant of ganglia latently infected with *wt*, KOS/29(LAT$^-$), and KOS/29Pr(LAT$^+$) viruses, and the signal was significantly stronger in samples of RNA isolated at 36 h postexplant. This result is consistent with the timing of viral DNA replication shown in Fig. 6 and 7. In trigeminal ganglia latently infected with *wt* 17*syn*$^+$, 17ΔPst-(LAT$^-$), or 17Pr(LAT$^+$) virus, productive-cycle transcripts such as α27 (U_L54) mRNA were also observed by 4 h following explant (Fig. 9B). In other experiments (not shown), we determined that no product was seen with use of the LAT-5′ or LAT-3′ primer set to amplify RNA isolated from ganglia latently infected with LAT$^-$ virus, the LAT 5′ signal intensity did not change over time in explants of ganglia latently infected with *wt* virus, and tissue recovery was shown to be essentially

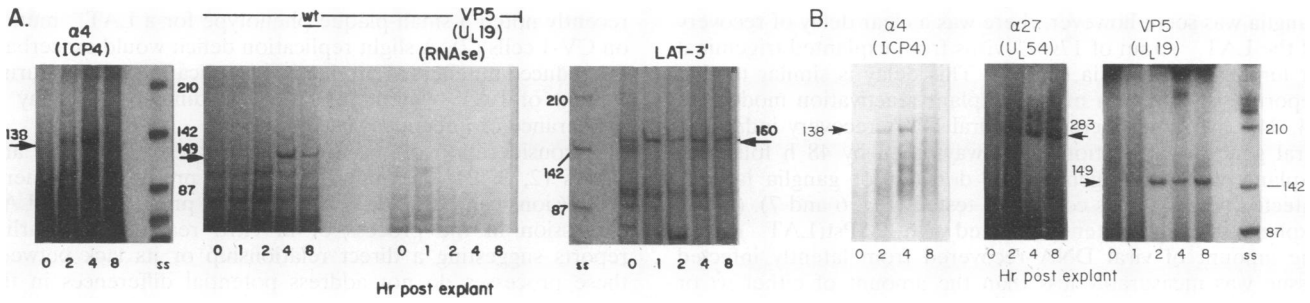

FIG. 8. Detection of HSV-1 transcripts by PCR amplification of RNA from latently infected murine lumbosacral ganglia cultured for various times following explant. Infection was with the KOS(M) strain of HSV-1. (A) Direct amplification. Primer sets are shown at the top. In the middle panel, products from an RNA sample treated with RNase are shown as a control to indicate the specificity of the direct PCR. (B) PCR-amplified oligo(dT)-primed cDNA. Details are as described for panel A; the primer sets used are shown at the top. Exposures were overnight at −70°C with intensifying screens. ss, size standards. Sizes are indicated in bases.

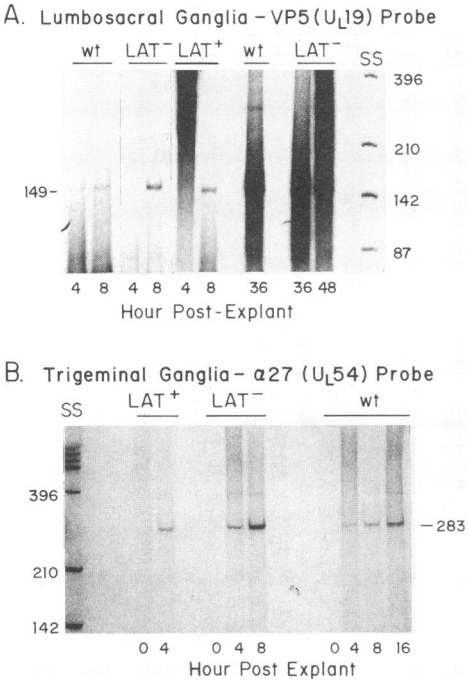

FIG. 9. Comparison of transcription in explants of ganglia latently infected with LAT$^+$ and LAT$^-$ derivatives of the KOS(M) and 17*syn*$^+$ strains of HSV-1. (A) Murine lumbosacral ganglia latently infected with *wt* KOS(M), KOS/29(LAT$^-$), and KOS/29Pr(LAT$^+$) viruses were explanted, and RNA was recovered at the times shown. Products of amplification of the primer set specific for VP5 (U_L19) mRNA are shown. (B) Murine trigeminal ganglia latently infected with *wt* 17*syn*$^+$, 17ΔPst(LAT$^-$), and 17Pr(LAT$^+$) viruses were explanted and incubated for the times shown. RNA was isolated and amplified with the α27 (U_L54) primer set. Exposures were overnight at −70°C with intensifying screens. SS, size standards. Sizes are indicated in bases.

equivalent in all samples by the use of the murine actin primer set.

DISCUSSION

The results of the experiments described in this report establish some of the basic molecular parameters of the murine in vitro explant model for HSV reactivation. Our results can be summarized as follows. (i) With *wt*, LAT$^-$, and LAT$^+$ rescuants of such mutants of HSV-1 strain KOS(M), no significant difference in the time of appearance of infectious virus in explant cultivation of latently infected murine lumbosacral ganglia was seen; however, there was a clear delay of recovery of the LAT$^-$ strain of 17*syn*$^+$ virus from explanted trigeminal or lumbosacral ganglia (Fig. 2). This delay is similar to that reported by others in murine explant reactivation models (3, 24, 34). (ii) A net increase in viral DNA recovery indicating viral genome replication was always seen by 48 h following explant of either trigeminal or dorsal root ganglia latently infected with all virus constructs tested (Fig. 6 and 7). (iii) In explants of ganglia latently infected with 17ΔPst(LAT$^-$) virus, the amount of viral DNA recovered from latently infected tissue was measurably less than the amount of either *wt* or LAT$^+$ virus. This slight reduction in efficiency of latent infection of murine ganglia with LAT$^-$ mutants of 17*syn*$^+$ virus readily correlates with the reduction in amount and delay in virus recovery seen in in vitro explant models. (iv) Transcription of productive-cycle genes could be detected within a few hours following explant cultivation of murine ganglia latently infected with all viruses tested. All of these results are consistent with a situation in which virus in a very few latently infected neurons rapidly enters the productive cascade following the insult of explant. This process is independent of LAT expression.

While viral DNA replication could readily be detected in as few as 10 productively infected cells by 8 h postinfection (Fig. 5), net viral DNA replication could not be seen at all before 24 h following explant of latently infected ganglia and more reliably only by 48 h (Fig. 6 and 7). The intensities of viral DNA signals in latently infected neurons compared with our quantitative analyses suggest that we were amplifying on the order of 1,000 copies of viral DNA at the onset of explant cultivation for each PCR (compare Fig. 4, 6, and 7). Given an upper limit of 10 viral genomes per latently infected neuron (36), this indicates that each amplified sample contains DNA from 100 or so latently infected cells. Immediate onset of productive replication in more than a very few of these cells would lead to an increase in viral DNA replication and recovery of infectious virus observed considerably earlier than the times actually seen.

As just described and on the basis of viral DNA recovery, we can estimate that explanted ganglia contain on the order of 1,000 copies of viral DNA in 100 cells at the onset of in vitro cultivation. Despite this, the intensities of PCR signals for productive-cycle viral transcripts observed in the first 8 to 16 h following explant were weak, of the same order of intensity as signals seen in amplification of samples containing RNA from fewer than 10 productively infected cells (compare Fig. 8 and 9A); only after 24 to 36 h are more intense RNA signals seen. Although intensity of PCR signal can be only roughly correlated with amounts of RNA in the infected cell, these data do, again, suggest that only a few cells produce RNA at early times following explant.

Although more complex scenarios can be posited, a significant factor in the delayed virus recovery phenotype seen with LAT$^-$ 17*syn*$^+$ virus in explanted latently infected ganglia may be due to the fewer number of latently infected cells undergoing productive infection at the earliest times because of a slightly lower efficiency of establishment of latent infection. We do not yet know the mechanistic basis for this lowered efficiency of establishment of latent infection in murine ganglia; it is not observed in the establishment of latent infections of rabbit ganglia (4). It may be that LAT$^-$ virus has a slight replication deficit in some cells during the acute phase of infection. In this regard, although data presented here and elsewhere indicate that any LAT-mediated function influencing replication efficiency is not observable in a number of assays of virus replication in vitro and in vivo, Block et al. have recently noted a small-plaque phenotype for a LAT$^-$ mutant on CV-1 cells (2). A slight replication deficit would exacerbate the reduced numbers of productively replicating centers during explant of LAT$^-$ latent infections, leading to the delay in appearance of infectious virus seen.

A consideration of the data accumulated here by us and others (2, 3, 24, 34) indicates that at present, no general conclusions can be made concerning the precise role of LAT expression in the process of in vitro reactivation. Earlier reports suggesting a direct relationship or its lack between these processes do not address potential differences in the efficiency of establishment of the latent infection by various LAT$^-$ and LAT$^+$ viruses. The data presented here indicate that the virus strain used can play a major role. In addition, the anatomical location of the neural tissue could also play a role, since Sawtell and Thompson reported a lowered efficiency of

latent infection of murine trigeminal ganglia with a murine hyperthermia-explant reactivation model using the same KOS/29(LAT$^-$) mutant used here (31). It should be noted, however, that Deshmane et al. have recently reported that the KOS/29(LAT$^-$) mutant reactivates equivalently to LAT$^+$ derivatives in explants of latently infected murine trigeminal ganglia (9); thus, the experimental system itself may also be critical. Further, although we cannot exclude dosage or the use of saline pretreatment as also being important, we do not favor this possibility because the levels of viral DNA isolated from ganglia latently infected with KOS(M)-derived virus mutants were similar to those seen in infections with 17*syn*$^+$ mutants (Table 4). We are in the process of examining strain-specific and dosage-dependent differences in greater detail.

As is shown in the accompanying report, the LAT-independent process of virus recovery in explanted murine ganglia displays both similarities with and differences from the LAT-dependent process occurring during induced reactivation in the rabbit model (4). It is not clear whether the different effects of LAT expression seen in these different animal models reflect fundamental differences between them or reflect a similar LAT-mediated restriction which has different manifestations in the two species. It is clear, however, that conclusions concerning the role of LAT expression in the reactivation of HSV from latency based on results with murine in vitro models should be generalized to in vivo models with caution.

ACKNOWLEDGMENTS

This research was supported by funds from National Multiple Sclerosis Society grant RG 1647-C-3, the W. M. Keck Foundation, and NIH grant AI06236 to J.G.S. and NIH grant CA11861 to E.K.W. D.C.B. is the recipient of a postdoctoral fellowship from the National Multiple Sclerosis Society. Further support was from the UCI Program in Animal Virology.

We thank Marcia Rice for technical assistance.

REFERENCES

1. **Alonso, S., A. Minty, Y. Bourlet, and M. E. Buckingham.** 1986. Comparison of three actin-coding sequences in the mouse: evolutionary relationships between the actin genes of warm-blooded vertebrates. J. Mol. Evol. **23:**11–22.
2. **Block, T. M., S. Deshmane, J. Masonis, J. Maggioncalda, T. Valyi-Nagy, and N. W. Fraser.** 1993. An HSV LAT null mutant reactivates slowly from latent infection and makes small plaques on CV-1 monolayers. Virology **192:**618–630.
3. **Block, T. M., J. G. Spivack, I. Steiner, S. Deshmane, M. T. McIntosh, R. P. Lirette, and N. W. Fraser.** 1990. A herpes simplex virus type 1 latency-associated transcript mutant reactivates with normal kinetics from latent infection. J. Virol. **64:**3417–3426.
4. **Bloom, D. C., G. B. Devi-Rao, J. M. Hill, J. G. Stevens, and E. K. Wagner.** 1994. Molecular analysis of herpes simplex virus type 1 during epinephrine-induced reactivation of latently infected rabbits in vivo. J. Virol. **68:**1283–1292.
5. **Bohenzky, R. A., A. G. Papavassiliou, I. H. Gelman, and S. J. Silverstein.** 1993. Identification of a promoter mapping within the reiterated sequences that flank the herpes simplex virus type 1 U_L region. J. Virol. **67:**632–642.
6. **Claoué, C. M. P., T. J. Hodges, J. M. Darville, T. J. Hill, W. A. Blyth, and D. L. Easty.** 1990. Possible latent infection with herpes simplex virus in the mouse eye. J. Gen. Virol. **71:**2385–2390.
7. **Cook, M. L., V. B. Bastone, and J. G. Stevens.** 1974. Evidence that neurons harbor latent herpes simplex virus. Infect. Immun. **9:**946–951.
8. **Croen, K. D.** 1991. Latency of the human herpesviruses. Annu. Rev. Med. **42:**61–67.
9. **Deshmane, S. L., M. Nicosia, T. Valyi-Nagy, L. T. Feldman, A. Dillner, and N. W. Fraser.** 1993. An HSV-1 mutant lacking the LAT TATA element reactivates normally in explant cocultivation. Virology **196:**868–872.
10. **Devi-Rao, G. B., S. A. Goodart, L. B. Hecht, R. Rochford, M. K. Rice, and E. K. Wagner.** 1991. The relationship between polyadenylated and nonpolyadenylated herpes simplex virus type 1 latency-associated transcripts. J. Virol. **65:**2179–2190.
11. **Dobson, A. T., F. Sedarati, G. B. Devi-Rao, W. M. Flanagan, M. J. Farrell, J. G. Stevens, E. K. Wagner, and L. T. Feldman.** 1989. Identification of the latency-associated transcript promoter by expression of rabbit beta-globin mRNA in mouse sensory nerve ganglia latently infected with a recombinant herpes simplex virus. J. Virol. **63:**3844–3851.
12. **Farrell, M. J., A. T. Dobson, and L. T. Feldman.** 1991. Herpes simplex virus latency-associated transcript is a stable intron. Proc. Natl. Acad. Sci. USA **88:**790–794.
13. **Farrell, M. J., J. M. Hill, T. P. Margolis, J. G. Stevens, E. K. Wagner, and L. T. Feldman.** 1993. The herpes simplex type 1 reactivation function lies outside the latency-associated transcript open reading frame. J. Virol. **67:**3653–3655.
14. **Feldman, L. T.** 1991. The molecular biology of herpes simplex virus latency, p. 223–244. *In* E. K. Wagner (ed.), Herpesvirus transcription and its regulation. CRC Press, Inc., Boca Raton, Fla.
15. **Gordon, Y. J., E. Romanowski, J. Harwick, J. Berman, L. Olsakovsky, and T. Araullo-Cruz.** 1990. The effect of alpha blockade on iontophoresis-induced ocular shedding of latent HSV-1 W in different host animals. Curr. Eye Res. **9:**1007–1014.
16. **Halford, W. P., W. Liu, and J. M. Hill.** Quantitative analysis of polymerase chain reaction products by a dot blot procedure. Submitted for publication.
17. **Hill, J. M., J. B. Dudley, Y. Shimomura, and H. E. Kaufman.** 1986. Quantitation and kinetics of adrenergic induced HSV-1 ocular shedding. Curr. Eye Res. **5:**241–246.
18. **Hill, J. M., Y. Haruta, and D. S. Rootman.** 1987. Adrenergically induced recurrent HSV-1 corneal epithelial lesions. Curr. Eye Res. **6:**1065–1071.
19. **Hill, J. M., F. Sedarati, R. T. Javier, E. K. Wagner, and J. G. Stevens.** 1990. Herpes simplex virus latent phase transcription facilitates in vivo reactivation. Virology **174:**117–125.
20. **Horikoshi, T., K. Danenberg, M. Volkandt, T. Stadlbauer, and P. V. Danenberg.** 1993. RNA template-specific polymerase chain reaction (RS-PCR). Methods Mol. Biol. **15:**169–188.
21. **Katz, J. P., E. T. Bodin, and D. M. Coen.** 1990. Quantitative polymerase chain reaction analysis of herpes simplex virus DNA in ganglia of mice infected with replication-incompetent mutants. J. Virol. **64:**4288–4295.
22. **Kinoshita, T., J. Imamura, H. Nagai, and K. Shimotohno.** 1992. Quantification of gene expression over a wide range by the polymerase chain reaction. Anal. Biochem. **206:**231–235.
23. **Kwon, B. S., L. P. Gangarosa, K. Green, and J. M. Hill.** 1982. Kinetics of ocular herpes simplex virus shedding induced by epinephrine iontophoresis. Invest. Ophthalmol. Visual Sci. **22:**818–821.
24. **Leib, D. A., C. L. Bogard, M. Kosz-Vnenchak, K. A. Hicks, D. M. Coen, D. M. Knipe, and P. A. Schaffer.** 1989. A deletion mutant of the latency-associated transcript of herpes simplex virus type 1 reactivates from the latent state with reduced frequency. J. Virol. **63:**2893–2900.
25. **Lowe, T., J. Sharefkin, S.-Q. Yang, and C. W. Dieffenback.** 1990. A computer program for selection of oligonucleotide primers for polymerase chain reactions. Nucleic Acids Res. **18:**1757–1761.
26. **McGeoch, D. J.** 1987. The genome of herpes simplex virus: structure, replication and evolution. J. Cell Sci. Suppl. **7:**67–94.
27. **Putney, S. D., W. O. Herlihy, and P. R. Schimmel.** 1983. A new troponin T and cDNA clones for 13 different muscle proteins found by shot-gun sequencing. Nature (London) **302:**718–721.
28. **Reed, L. H., and H. Muench.** 1938. A simple method of estimating fifty percent endpoints. Am. J. Hyg. **27:**493–497.
29. **Rice, M. K., G. B. Devi-Rao, and E. K. Wagner.** 1993. Latent phase transcription by alphaherpesviruses, p. 305–324. *In* K. W. Adolph (ed.), Genome research in molecular medicine and virology. Academic Press, Orlando, Fla.
30. **Rong, B.-L., D. Pavan-Langston, Q.-P. Weng, R. Martinez, J. M. Cherry, and E. C. Dunkel.** 1991. Detection of herpes simplex virus thymidine kinase and latency-associated transcript gene sequences in human herpetic corneas by polymerase chain reaction amplifi-

cation. Invest. Ophthalmol. Visual Sci. **32:**1808–1815.
31. **Sawtell, N. M., and R. L. Thompson.** 1992. Herpes simplex virus type 1 latency-associated transcription unit promotes anatomical site-dependent establishment and reactivation from latency. J. Virol. **66:**2157–2169.
32. **Sawtell, N. M., and R. L. Thompson.** 1992. Rapid in vivo reactivation of herpes simplex virus in latently infected murine ganglionic neurons after transient hyperthermia. J. Virol. **66:**2150–2156.
33. **Stanberry, L. R.** 1992. Pathogenesis of herpes simplex virus infection and animal models for its study. Curr. Top. Microbiol. Immunol. **179:**15–30.
34. **Steiner, I., J. G. Spivack, R. P. Lirette, S. M. Brown, A. R. MacLean, J. H. Subak-Sharpe, and N. W. Fraser.** 1989. Herpes simplex virus type 1 latency-associated transcripts are evidently not essential for latent infection. EMBO J. **8:**505–511.
35. **Stevens, J. G.** 1975. Latent herpes simplex virus and the nervous system. Curr. Top. Microbiol. Immunol. **70:**31–50.
36. **Stevens, J. G.** 1989. Human herpesviruses: a consideration of the latent state. Microbiol. Rev. **53:**318–332.
37. **Stevens, J. G.** 1990. Transcripts associated with herpes simplex virus latency. Adv. Exp. Med. Biol. **278:**199–204.
38. **Stevens, J. G., and M. L. Cook.** 1971. Latent herpes simplex virus in spinal ganglia of mice. Science **173:**843–845.
39. **Stevens, J. G., E. K. Wagner, G. B. Devi-Rao, M. L. Cook, and L. T. Feldman.** 1987. RNA complementary to a herpesvirus alpha gene mRNA is prominent in latently infected neurons. Science **235:** 1056–1059.
40. **Thompson, R. L., M. L. Cook, G. B. Devi-Rao, E. K. Wagner, and J. G. Stevens.** 1986. Functional and molecular analysis of the avirulent wild-type herpes simplex virus type 1 strain KOS. J. Virol. **58:**203–211.
41. **Thompson, R. L., G. B. Devi-Rao, J. G. Stevens, and E. K. Wagner.** 1985. Rescue of a herpes simplex virus type 1 neurovirulence function with a cloned DNA fragment. J. Virol. **55:**504–508.
42. **Thompson, R. L., E. K. Wagner, and J. G. Stevens.** 1983. Physical location of a herpes simplex virus type-1 gene function(s) specifically associated with a 10 million-fold increase in HSV neurovirulence. Virology **131:**180–192.
43. **Trousdale, M. D., I. Steiner, J. G. Spivack, S. L. Deshmane, S. M. Brown, A. R. MacLean, J. H. Subak-Sharpe, and N. W. Fraser.** 1991. In vivo and in vitro reactivation impairment of a herpes simplex virus type 1 latency-associated transcript variant in a rabbit eye model. J. Virol. **65:**6989–6993.
44. **Wagner, E. K.** 1991. Herpesvirus transcription—general aspects, p. 1–15. *In* E. K. Wagner (ed.), Herpesvirus transcription and its regulation. CRC Press, Inc., Boca Raton, Fla.
45. **Wagner, E. K.** The HSV-1 latency gene. *In* Y. Becker and G. Darai (ed.), Frontiers of virology, vol. 3, in press. Springer-Verlag, Heidelberg, Germany.
46. **Wagner, E. K., G. B. Devi-Rao, L. T. Feldman, A. T. Dobson, Y. F. Zhang, W. M. Flanagan, and J. G. Stevens.** 1988. Physical characterization of the herpes simplex virus latency-associated transcript in neurons. J. Virol. **62:**1194–1202.
47. **Wagner, E. K., W. M. Flanagan, G. B. Devi-Rao, Y. F. Zhang, J. M. Hill, K. P. Anderson, and J. G. Stevens.** 1988. The herpes simplex virus latency-associated transcript is spliced during the latent phase of infection. J. Virol. **62:**4577–4585.
48. **Yeh, Z., and P. A. Schaffer.** 1993. A novel class of transcripts expressed with late kinetics in the absence of ICP4 spans the junction between the long and short segments of the herpes simplex virus type 1 genome. J. Virol. **67:**7373–7382.